Published in final edited form as:
Brain Res. 2004 April 2; 1003(1-2): 54–60. doi:10.1016/j.brainres.2003.10.076.

Morphological differences between planes of section do not influence the electrophysiological properties of identified rat dorsal motor nucleus of the vagus neurons

Isabel Martinez-Peña y Valenzuela[a], **Kirsteen N. Browning**[a], and **R. Alberto Travagli**[a,b,*]

[a] Department of Internal Medicine–Gastroenterology, University of Michigan, Ann Arbor, MI, USA

[b] Department of Physiology, University of Michigan, Ann Arbor, MI, USA

Abstract

Recent cytoarchitectonic studies have shown that the dorsal motor nucleus of the vagus (DMV) comprises neurons with different morphological features. Our own studies, conducted in horizontal brainstem slices, have shown that DMV neurons projecting to stomach areas can be distinguished from neurons projecting to the intestine on the basis of their electrophysiological as well as morphological properties. The majority of the in vitro experimental investigations, however, have been conducted on coronal brainstem slices. The aim of the present study was to assess whether the electrophysiological properties of DMV neurons are due to intrinsic membrane properties of the neurons or are dependent upon the plane of section, i.e., coronal vs. horizontal, in which the brainstem is cut. The fluorescent retrograde tracer DiI was applied to either the stomach or intestine of rats. Whole cell recordings were subsequently made from labeled DMV neurons in thin brainstem slices sectioned in either the horizontal or coronal plane. In the horizontal plane, both the somata and the dendritic tree of gastric-projecting neurons were smaller than intestinal-projecting neurons. In the coronal plane, however, apart from a smaller soma diameter in gastric-projecting neurons, morphological differences were not found between the groups. The electrophysiological differences observed between the groups were, however, consistent in both planes of section, that is, intestinal-projecting neurons had larger and longer afterhyperpolarization (AHP) as well as slower frequency–responses to depolarizing stimuli than gastric-projecting neurons. Our data suggest that intrinsic rather than morphological features govern the electrophysiological characteristics of DMV neurons.

Keywords

Gastrointestinal; Stomach; Intestine; Dorsal vagal complex; Vagus

1. Introduction

The dorsal motor nucleus of the vagus (DMV) contains the parasympathetic motoneurons that innervate the majority of the gastrointestinal (GI) tract [12,24,26]. Several previous studies demonstrated the morphological heterogeneity of DMV neurons [4,9,11,14,15,27]. Indeed, the extent and orientation of the DMV neuronal arbor has been shown to vary along both the rostro–caudal and the medio–lateral boundaries of the nucleus [11]. Jarvinen and

*Corresponding author. Department of Internal Medicine–Gastroenterology, University of Michigan, 6520 MSRB I, 1150 West Medical Center Drive, Ann Arbor, MI 48109-0682, USA. Tel.: +1-734-615-8517; fax: +1-734-763-2535. Travagli@umich.edu (R.A. Travagli).

Powley [15], however, suggested that the DMV neuronal population might represent variations of a continuum.

Our own studies, conducted in horizontal brainstem slices, have shown that DMV neurons identified as projecting to discrete gastrointestinal areas can also be distinguished on the basis of their electrophysiological properties [4]. The majority of the in vitro experimental investigations, however, have been conducted on coronal brainstem slices [5–7,20,22,23,25].

Because the plane in which the brainstem slice is sectioned may preserve preferentially neurons of a particular soma size and as portions of the dendritic arbor would be better preserved in horizontal rather than in coronal slices [11], it is unclear whether the aforementioned morphological differences influence the basic electrophysiological properties of DMV neurons. Furthermore, pharmacological responses distinguish subgroups of DMV neurons [1–3,6,8,16,17], raising the possibility that the observed differences could be determined by a discrete distribution of channels and receptors on the dendritic arbor of the DMV neurons.

The aim of the present study was, thus, to assess whether the electrophysiological properties of DMV cells are determined by the intrinsic membrane properties of the neurons or are dependent upon the plane of section, i.e., coronal vs. horizontal.

2. Materials and methods

Rat pups of either sex (10–12 days old) were anesthetized deeply with Halothane® before an abdominal laparotomy was performed. Crystals of the retrograde tracer DiI were applied to the stomach (along the greater curvature of either the gastric fundus, corpus or antrum/pylorus) or intestine (either at the antimesenteric border of the duodenum or at the level of the ileo–cecal junction) as described previously [4]; a fast hardening epoxy resin was then used to confine the tracer to the application site. The resin was allowed to harden before the wound was sutured and the rat was allowed to recover for 10–15 days. On the day of the experiment, the animal was anesthetized and killed by severing the major blood vessels in the chest; the brainstem was removed and cut into 200-μm-thick sections in either the horizontal or coronal plane [4,25]. Slices were equilibrated for a minimum of 1 h at 35 ±1 °C in Krebs' solution (in mM: 126 NaCl, 25 $NaHCO_3$, 2.5 KCl, 1.2 $MgCl_2$, 2.4 $CaCl_2$, 1.2 NaH_2P0_4 and 11 dextrose) maintained at pH 7.4 by bubbling with O_2 –CO_2 (95–5%). A single slice was then placed in a custom-made perfusion chamber (volume 500μl), kept in place by a nylon mesh and maintained at 35 ±1 °C by continual perfusion with warmed oxygenated Krebs' solution at a rate of 2.5 ml/min.

Retrogradely labeled DMV neurons were identified prior to electrophysiological recordings using a Nikon E600-FS microscope equipped with TRITC epifluorescent filters. Once detected, the neurons' position was confirmed under bright field illumination using DIC (Nomarski) optics. Whole cell recordings were performed with patch pipettes (3–8 MΩ) filled with a potassium gluconate intracellular solution (in mM: K-gluconate 128, 10 KCl, 0.3 $CaCl_2$, 1 $MgCl_2$, 10 Hepes, 1 EGTA, 2 ATP, 0.25 GTP adjusted to pH 7.35 with KOH) using a single-electrode voltage clamp amplifier (Axoclamp 2B, Axon Instr., Union City, CA). Data were filtered at 2 kHz, digitized via a Digidata 1320 interface (Axon Instr.), acquired, stored and analysed on an IBM PC utilizing pClamp8 software (Axon Instr.). Only those recordings having a series resistance < 15 MΩ were used. A single action potential (AP) was obtained from neurons held at −60 mV and injected with a 5–30-ms-long pulse of depolarizing current sufficient to evoke a single action potential at its offset. For a neuronal recording to be accepted, the membrane had to be stable at the holding potential, the action

potential evoked following injection of DC had to have an amplitude of at least 60 mV, and the membrane had to return to baseline at the end of the afterhyperpolarization (AHP).

Electrophysiological properties measured included the membrane input resistance (measured from the current deflection obtained by stepping the membrane from −50 to −60 mV), the duration of the action potential measured at the threshold, the amplitude and duration of the afterhyperpolarization following the firing of a single action potential and the frequency of action potential firing, expressed as pulses per second, in response to depolarizing current pulses of 400 ms duration and intensities ranging from 30 to 270 pA in step increments. At the end of recording, Neurobiotin® (2.5% w/v) was injected into the neuron (0.3 nA, 600 ms duration depolarizing pulse every 2 s) to permit postfixation reconstruction of the neuronal morphology. The avidin–horseradish peroxidase technique used to develop the Neurobiotin stain and the protocol used for reconstruction of the neuronal morphology have been described in detail previously [4]. Neuronal reconstructions were performed using Neurolucida® software (Microbrightfield, Williston, VT).

Results are expressed as means ±S.E.M. Intergroup comparisons were analysed with one-way ANOVA followed by Student's grouped *t* test. Significance was defined as $P < 0.05$.

3. Results

Whole cell recordings were made from a total of 205 retrogradely labeled DMV neurons. Of those neurons, 127 projected to the stomach (48 to the fundus, 24 in horizontal section, 24 in coronal section; 44 to the corpus, 23 horizontal, 21 coronal; 35 to the antrum/pylorus, 18 horizontal, 17 coronal) and 78 projected to the intestine (38 to the duodenum, 18 in horizontal section, 20 in coronal section; 40 to the caecum, 16 horizontal, 24 coronal).

Fundus-, corpus- or duodenum-projecting neurons in slices cut in the coronal plane did not show statistically significant differences in their basic electrophysiological properties when compared to neurons projecting to the same areas from slices cut in the horizontal plane. Significant differences were observed, however, in the afterhyperpolarization (AHP) amplitude of caecum- and antrum/pylorus-projecting neurons and in the action potential (AP) duration of caecum-projecting neurons when comparing neurons from slices cut in the horizontal vs. coronal plane. In detail, the AHP amplitude in caecum-projecting neurons was 19.8 ±0.9 and 23.4 ±1.2 mV while the AHP amplitude in antrum/pylorus neurons was 18.9 ±0.9 and 15.9 ±1.0 mV in the coronal and in the horizontal plane, respectively ($P < 0.05$). Furthermore, differences were observed in the action potential duration in caecum-projecting neurons from slices in the coronal and horizontal planes (4.3 ±0.2 and 3.3 ±0.2 ms, respectively; $P < 0.05$).

The electrophysiological data are summarized in Table 1.

Intergroup differences between discrete GI regions were observed both in the horizontal as well as in the coronal plane of section; we do not, however, report these comparisons in the present manuscript but refer the reader to our previous manuscript in which we conducted a thorough analysis of the properties of neurons from slices cut in the horizontal plane [4].

We then pooled the data in two groups comprising gastric- or intestinal-projecting neurons. As with the intragroup comparisons, the plane of section did not influence significantly the basic electrophysiology of gastric- or intestinal-projecting neurons. When the electrophysiological properties of gastric-projecting neurons were compared to those of intestinal-projecting neurons, however, the differences were statistically significant, independently from the plane in which the slices were cut. For example, following a single action potential the AHP was significantly smaller and faster in gastric-than in intestinal-

projecting neurons; in fact, in the coronal plane, the AHP amplitude was 17.6 ±0.46 mV and the AHP time constant of decay (τ) was 58.2 ±3.42 ms in gastric-projecting neurons (N = 60), while in intestinal-projecting neurons the AHP amplitude and the AHP τ were 21.2 ±0.7 mV and 87.4 ±4.8 ms, respectively (N = 44; $P < 0.05$ for both; Fig. 1). In addition, the frequency of action potential firing in response to step depolarizing current injection was markedly different between the neuronal groups independently from the plane of section of the slice. In fact, gastric-projecting neurons had faster frequency responses than intestinal-projecting neurons (Fig. 2).

The electrophysiological data are summarized in Table 2.

At the end of the electrophysiology experiment, all the neurones were filled with Neurobiotin® to allow postfixation morphological reconstruction. We were able to assess the morphological properties of 125 identified, neurobiotin-filled DMV neurons. Of those neurons, 72 projected to the stomach (28 to the fundus, 18 in horizontal section, 10 in coronal section; 25 to the corpus, 19 horizontal, 6 coronal; 16 to the antrum/pylorus, 12 horizontal, 4 coronal) and 53 projected to the intestine (26 to the duodenum, 19 in horizontal section, 7 in coronal section; 27 to the caecum, 12 in horizontal section, 15 in coronal section).

When sectioned in the horizontal plane, intestinal-projecting neurons had larger soma diameters and areas as well as larger total cell volumes and a larger number of branch segments compared to gastric-projecting neurons. Conversely, the only differences we observed between gastric- and intestinal-projecting neurons from slices cut in the coronal plane was the soma diameter and the soma form factor (a measure of circularity for which a value of 1 indicates a perfect circle and 0 indicates a line; form factor = $4\pi a \times 1/p^2$, where a is the soma area and p is the perimeter of the soma in the horizontal plane; Fig. 3 and Table 3).

Interestingly, intestinal-projecting neurons from slices cut in the different planes were significantly different when considering the soma volume and area, as well as the form factor, the number of segments and the branch order (Table 3).

The morphological properties of the neurons in relation to their projection and plane of section are summarized in Table 3.

4. Discussion

In the present study, we provide evidence that the electrophysiological properties of DMV neurons are determined by intrinsic membrane properties rather than by morphological characteristic determined by the plane of section.

Our conclusions are based upon the following experimental evidence.

Intestinal-projecting neurons from slices cut in the horizontal or coronal plane display differences in soma volume, area and form factor, number of segments and branch order. Despite these morphological differences, the basic electrophysiological membrane properties of neurons obtained from slices cut in the horizontal plane did not differ from those of neurons obtained from slices cut in the coronal plane.

The morphological differences between gastric- and intestinal-projecting neurons from slices cut in the horizontal plane were not observed when the neurons were obtained from slices cut in the coronal plane (apart from differences in soma diameter and form factor). The electrophysiological differences observed between horizontally sectioned gastric-and

intestinal-projecting neurons were preserved, however, when compared to those of neurons obtained from slices cut in the coronal plane.

Our previous studies have demonstrated that, when in the horizontal plane of section, preganglionic parasympathetic motoneurons innervating the gastrointestinal tract can be distinguished in their morphological and electrophysiological properties as per their target organ of innervation [4]. Specifically, gastric-projecting neurons have smaller and shorter AHPs than intestinal-projecting neurons and, correspondingly, have higher frequencies of action potential firing. The current study highlighted these differences in electrophysiological properties and found that such differences were apparent irrespective of the plane in which the brainstem had been sectioned prior to recording. For example, the electrophysiological properties of gastric-projecting neurons sectioned in the coronal plane were indistinguishable from those sectioned in the horizontal plane. As with neurons sectioned in the horizontal plane, although, the electrophysiological properties of coronally sectioned gastric-projecting neurons differed from those of intestinal-projecting neurons; gastric-projecting neurons had a similarly smaller and shorter AHP and a faster frequency of action potential firing than intestinal-projecting neurons.

Several previous studies demonstrated the morphological heterogeneity of DMV neurons [4,9,11,14,15,27]. Indeed, the extent and orientation of the DMV neuronal arbor has been shown to vary along both the rostro–caudal and the medio–lateral boundaries of the nucleus [11]. In our previous study, in which brainstem sections were cut in the horizontal plane, intestinal-projecting neurons were also found to have larger soma diameters and areas, larger total cell volumes and a larger number of branch segments than gastric-projecting neurons [4]. The present study confirmed these findings, but the present data also indicate that, when cut in the coronal plane, intestinal-projecting neurons differ from gastric-projecting neurons only in having a larger soma diameter and a lower soma form factor. Gastric-projecting neurons were not found to differ morphologically when viewed either in horizontal or coronal sections. Because intestinal-projecting neurons display morphological differences when cut in different planes (soma volume, soma area, form factor, number of segments and branch order), our data suggest that the soma of intestinal-projecting neurons are oriented preferentially in the rostro–caudal plane. Conversely, no significant differences can be observed in the orientation of gastric-projecting neurons.

Our data differ from the data presented by Jarvinen and Powley [15]. In fact, these authors reported four discrete morphological neuron types; however, they did not report differences in the location of the DMV neuronal subtypes and suggested that “in any motor neuron pool located within specific regions of the dorsal motor nucleus are ensembles comprised of all four basic classes of cells”. Several reasons may underlie this apparent discrepancy between Jarvinen and Powley’s and the present data. Firstly, from a technical standpoint, it is difficult to compare morphological results obtained by different groups utilizing different fixation and sampling techniques. Furthermore, in their study, Jarvinen and Powley collected their results from DMV neurons labeled following intraperitoneal injection of fluorogold, a technique utilized that labels all DMV neurons innervating subdiaphragmatic viscera [13,19,28]. By doing so, Jarvinen and Powley might have skewed their analysis toward gastric-projecting DMV neurons. In fact, gastric-projecting neurons project to the viscera via three of the five subdiaphragmatic vagal branches, which originate in the medial two-third of the DMV [10,18,21]. Our sampling technique, instead, focuses on DMV neurons that are identified as projecting to specific visceral targets, and it is more prone to uncover, if present, morphological differences between anatomically distinct neuronal subgroups.

In conclusion, we have shown that the electrophysiological characteristics of identified gastrointestinal-projecting DMV neurons are maintained despite the plane of section, and, in the case of intestinal-projecting neurons, despite differences in morphological properties. In fact, although, in the present study, we did not measure the specific contribution of the dendrities to the overall whole cell current, our data indicate that the electrophysiological differences are not artifacts determined by the extent of dendritic arborization but rather are intrinsic to the cell body.

Acknowledgments

Supported by NIH-NIDDK grant #DK55530. We would like to thank F. Holly Coleman, B.S., for excellent technical assistance in the neuronal reconstructions and Dr. R.C. Rogers for comments on previous versions of the manuscript. We wish to acknowledge the support and encouragement of Cesare M. Travagli.

References

1. Browning KN, Travagli RA. Characterization of the in vitro effects of 5-hydroxytryptamine (5HT) on identified neurones of the rat dorsal motor nucleus of the vagus (DMV). Br J Pharmacol. 1999; 128:1307–1315. [PubMed: 10578146]
2. Browning KN, Travagli RA. Mechanism of action of baclofen in rat dorsal motor nucleus of the vagus. Am J Physiol: Gasterointest Liver Physiol. 2001; 280:G1106–G1113.
3. Browning KN, Travagli RA. Neuropeptide Y and peptide YY inhibit excitatory synaptic transmission in the rat dorsal motor nucleus of the vagus. J Physiol. 2003; 549:775–785. [PubMed: 12730340]
4. Browning KN, Renehan WE, Travagli RA. Electrophysiological and morphological heterogeneity of rat dorsal vagal neurones which project to specific areas of the gastrointestinal tract. J Physiol. 1999; 517:521–532. [PubMed: 10332099]
5. Browning KN, Kalyuzhny AE, Travagli RA. Opioid peptides inhibit excitatory but not inhibitory synaptic transmission in the rat dorsal motor nucleus of the vagus. J Neurosci. 2002; 22:2998–3004. [PubMed: 11943802]
6. Davis SF, Williams KW, Xu W, Glatzer NR, Smith BN. Selective enhancement of synaptic inhibition by hypocretin (orexin) in rat vagal motor neurons: implications for autonomic regulation. J Neurosci. 2003; 23:3844–3854. [PubMed: 12736355]
7. Dean JB, Huang RQ, Erlichman JS, Southard TL, Hellard DT. Cell–cell coupling occurs in dorsal medullary neurons after minimizing anatomical-coupling artifacts. Neuroscience. 1997; 80:21–40. [PubMed: 9252218]
8. Emch GS, Hermann GE, Rogers RC. Tumor necrosis factor-alpha inhibits physiologically identified dorsal motor nucleus neurons in vivo. Brain Res. 2002; 951:311–315. [PubMed: 12270510]
9. Fogel R, Zhang X, Renehan WE. Relationships between the morphology and function of gastric and intestinal distention-sensitive neurons in the dorsal motor nucleus of the vagus. J Comp Neurol. 1996; 364:78–91. [PubMed: 8789277]
10. Fox EA, Powley TL. Longitudinal columnar organization within the dorsal motor nucleus represents separate branches of the abdominal vagus. Brain Res. 1985; 341:269–282. [PubMed: 4041795]
11. Fox EA, Powley TL. Morphology of identified preganglionic neurons in the dorsal motor nucleus of the vagus. J Comp Neurol. 1992; 322:79–98. [PubMed: 1385488]
12. Gillis, RA.; Quest, JA.; Pagani, FD.; Norman, WP. Control centers in the central nervous system for regulating gastrointestinal motility. In: Wood, JD., editor. Handbook of Physiology. Section 6 The Gastrointestinal System Motility and Circulation. Vol. 1. American Physiological Society; Bethesda, MD: 1989. p. 621-683.
13. Guo JJ, Browning KN, Rogers RC, Travagli RA. Catecholaminergic neurons in rat dorsal motor nucleus of vagus project selectively to gastric corpus. Am J Physiol: Gasterointest Liver Physiol. 2001; 280:G361–G367.

14. Huang X, Tork I, Paxinos G. Dorsal motor nucleus of the vagus nerve: a cyto- and chemoarchitectonic study in the human. J Comp Neurol. 1993; 330:158–182. [PubMed: 7684048]
15. Jarvinen MK, Powley TL. Dorsal motor nucleus of the vagus neurons: a multivariate taxonomy. J Comp Neurol. 1999; 403:359–377. [PubMed: 9886036]
16. Lewis MW, Travagli RA. Effects of substance P (SP) on identified neurons of the rat dorsal motor nucleus of the vagus (DMV). Am J Physiol: Gasterointest Liver Physiol. 2001; 281:G164–G172.
17. Lewis MW, Hermann GE, Rogers RC, Travagli RA. In vitro and in vivo analysis of the effects of corticotropin releasing factor on rat dorsal vagal complex. J Physiol. 2002; 543:135–146. [PubMed: 12181286]
18. Norgren R, Smith GP. Central distribution of subdiaphragmatic vagal branches in the rat. J Comp Neurol. 1988; 273:207–223. [PubMed: 3417902]
19. Powley TL, Fox EA, Berthoud HR. Retrograde tracer technique for assessment of selective and total subdiaphragmatic vagotomies. Am J Physiol. 1987; 253:R361–R370. [PubMed: 3618835]
20. Sah P. Different calcium channels are coupled to potassium channels with distinct physiological roles in vagal neurons. Proc R Soc Lond. 1995; 260:105–111.
21. Shapiro RE, Miselis RR. The central organization of the vagus nerve innervating the stomach of the rat. J Comp Neurol. 1985; 238:473–488. [PubMed: 3840183]
22. Trapp S, Luekermann M, Brooks PA, Ballanyi K. Acidosis of rat dorsal vagal neurons in situ during spontaneous and evoked activity. J Physiol. 1996; 496:695–710. [PubMed: 8930837]
23. Travagli RA, Gillis RA. Hyperpolarization-activated currents I_H and I_{KIR}, in rat dorsal motor nucleus of the vagus neurons in vitro. J Neurophysiol. 1994; 71:1308–1317. [PubMed: 8035216]
24. Travagli RA, Rogers RC. Receptors and transmission in the brain–gut axis: potential for novel therapies: V. Fast and slow extrinsic modulation of dorsal vagal complex circuits. Am J Physiol: Gasterointest Liver Physiol. 2001; 281:G595–G601.
25. Travagli RA, Gillis RA, Rossiter CD, Vicini S. Glutamate and GABA-mediated synaptic currents in neurons of the rat dorsal motor nucleus of the vagus. Am J Physiol. 1991; 260:G531–G536. [PubMed: 1672243]
26. Travagli RA, Hermann GE, Browning KN, Rogers RC. Musings on the wanderer: what's new in our understanding of vago – vagal reflexes?: III. Activity-dependent plasticity in vago – vagal reflexes controlling the stomach. Am J Physiol: Gasterointest, Liver Physiol. 2003; 284:G180–G187.
27. Zhang X, Fogel R, Renehan WE. Physiology and morphology of neurons in the dorsal motor nucleus of the vagus and the nucleus of the solitary tract that are sensitive to distension of the small intestine. J Comp Neurol. 1992; 323:432–448. [PubMed: 1281172]
28. Zheng ZL, Rogers RC, Travagli RA. Selective gastric projections of nitric oxide synthase-containing vagal brainstem neurons. Neuroscience. 1999; 90:685–694. [PubMed: 10215170]

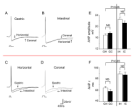

Fig. 1.

Representative traces showing that the amplitude and kinetic of decay (τ) of the action potential afterhyperpolarization (AHP) of gastric-projecting neurons (A) are smaller and faster than those of intestinal-projecting neurons (B). The differences in the action potential characteristics between groups were maintained independently of the plane of section; however, no differences were observed within the groups when the plane of section, i.e., neurons from horizontal (C) or coronal (D) cut slices, was considered. Data highlighting the differences in AHP amplitude and τ are summarized in (E) and (F), respectively. GH: gastric-projecting neurons from slices cut in the horizontal plane; GC: gastric-projecting neurons from slices cut in the coronal plane; IH: intestinal-projecting neurons from slices cut in the horizontal plane; IC: intestinal-projecting neurons from slices cut in the coronal plane. Holding potential = −55 mV.

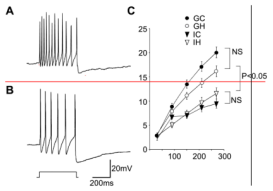

Fig. 2.

Representative traces showing repetitive action potentials following injection of a 400-ms-long DC pulse (270 pA) in neurons from slices cut in the coronal plane. Note the faster frequency of firing in the gastric-projecting neuron (A) compared to the intestinal-projecting neuron (B). The summarized frequency–response curves for DMV neurons from slices cut in the different planes (C) show that the frequency–response curve within the gastric- or intestinal-projecting neurons is similar irrespective of the plane in which the slices were cut. However, the frequency–response to DC injection differed between gastric and intestinal-projecting neurons. Holding potential = −55 mV, GC and GH: gastric-projecting neurons in the coronal and horizontal plane, respectively; IC and IH: intestinal-projecting neurons in the coronal and horizontal plane, respectively.

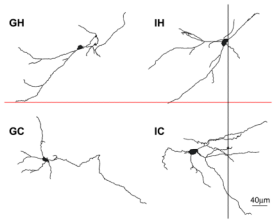

Fig. 3.

Computer-generated reconstruction of representative neurons in the different planes of section. See Table 3. GC and GH: gastric-projecting neurons in the coronal and horizontal plane, respectively; IC and IH: intestinal-projecting neurons in the coronal and horizontal plane, respectively.

Table 1

Summary of basic electrophysiological properties

	R_{imp} (MΩ)	AP duration (ms)	AHP amplitude (mV)	AHP τ (ms)	Number of AP/s (30 pA)	Number of AP/s (270 pA)
Fundus						
Horizontal	418 ±40	3.1 ±0.1	16.9 ±0.6	68.5 ±4.3	3.7 ±0.7	17.0 ±2.0
Coronal	389 ±31	3.4 ±0.2	16.7 ±0.7	56.9 ±5.4	3.1 ±0.9	19.4 ±1.7
Corpus						
Horizontal	293 ±21	3.0 ±0.2	17.7 ±0.8	68.8 ±4.2	3.0 ±0.3	15.0 ±1.4
Coronal	359 ±31	3.2 ±0.2	17.7 ±0.8	61.9 ±6.7	3.9 ±0.7	17.8 ±2.3
A/P						
Horizontal	272 ±30	2.9 ±0.1	15.9 ±1.0	53.2 ±3.9	2.9 ±0.5	17.6 ±2.2
Coronal	320 ±27	2.7 ±0.2	18.9 ±0.9*	55.1 ±5.6	3.9 ±0.5	22.9 ±1.9
Duodenum						
Horizontal	301 ±32	2.8 ±0.1	21.6 ±0.8	84.1 ±6.5	3.0 ±0.4	12.4 ±1.4
Coronal	324 ±32	2.6 ±0.1	23.0 ±0.9	73.4 ±3.9	3.1 ±0.9	12.5 ±2.3
Caecum						
Horizontal	340 ±32	3.3 ±0.2	23.4 ±1.2	94.9 ±5.8	2.1 ±0.6	9.6 ±2.2
Coronal	373 ±50	4.3 ±0.2*	19.8 ±0.9*	98.5 ±7.3	3.1 ±0.3	7.7 ±0.8

*$P < 0.05$ vs. horizontal.

Table 2

Summary of electrophysiological properties

	Gastric-projecting neurons		Intestinal-projecting neurons	
	Coronal	Horizontal	Coronal	Horizontal
	N = 41–60[a]	*N* = 40–63[a]	*N* = 23–44[a]	*N* = 20–34[a]
Input resistance (MΩ)	360 ±17.4	315 ±18.1	333 ±27.3	313 ±24.3
Action potential duration (ms)	3.2 ±0.11	3.0 ±0.09	3.6 ±0.20* IH	3.0 ±0.14
Afterhyperpolarization amplitude (mV)	17.6 ±0.46* IC	16.9 ±0.46* IH	21.2 ±0.70* GC	22.5 ±0.75* GH
Afterhyperpolarization duration (ms)	58.2 ±3.42* IC	64.2 ±2.57* IH	87.4 ±4.77* GC	89.3 ±4.42* GH
Number of action potentials at 30 pA	3.0 ±0.32	3.2 ±0.27	2.2 ±0.31	2.8 ±0.33
Number of action potentials at 270 pA	20.1 ±1.14*GH, IC	16.2 ±1.12*GC, IH	9.5 ±0.93*GC	11.6 ±1.17*GH

[a]Because not all the measures could be obtained from all the cells, the range of values is reported.

*$P < 0.05$ vs. gastric (G) or intestinal (I) in coronal (C) or horizontal (H) plane of section.

Table 3

Summary of morphological properties

	Gastric-projecting neurons		Intestinal-projecting neurons	
	Coronal	Horizontal	Coronal	Horizontal
	N = 15–20[a]	*N* = 45–51[a]	*N* = 11–22[a]	*N* = 25–30[a]
Soma volume (μm^3)	3029 ±360	3200 ±217*IH	2185 ±386*IH	4834 ±360
Soma area (μm^2)	314 ±19.4	327 ±15.5* IH	292 ±21* IH	403 ±24.0
Soma diameter (μm)	19.8 ±0.65* IC	20.2 ±0.47* IH	24.1 ±1.25	22.3 ±0.68
Form factor (0 = line, 1 = circle)	0.83 ±0.01* IC	0.79 ±0.02	0.71 ±0.02* IH	0.82 ±0.02
Number of segments	19 ±2.1	19 ±0.8* IH	15 ±1.4* IH	23 ±1.5
Branch order	4.1 ±0.47	4.7 ±0.19	4.0 ±0.25* IH	4.9 ±0.25
Dendritic *x*-plane (μm)	352 ±34.2	375 ±24.1	367 ±27.5	420 ±28.1
Dendritic *y*-plane (μm)	198 ±16.6	317 ±22.1	235 ±23.4	335 ±34.7
Segment length (μm)	116 ±8.9	111 ±4.2	133 ±10.8	116 ±6.5

[a] Because not all the measures could be obtained from all the cells, the range of values is reported.

* $P < 0.05$ vs. gastric (G) or intestinal (I) in coronal (C) or horizontal (H) plane of section.